

## Separation of Proteins Mixture in Hollow Fiber Flow Field-Flow Fractionation

Se-Jong Shin, Hyun-Hee Nam, Byoung-Ryul Min,\* Jin-Won Park, Ik-Sung An, and Kangtaek Lee

Department of Chemical Engineering, Yonsei University, Seoul 120-749, Korea

Received May 28, 2003

Flow field-flow fractionation (FIFFF) is a technology to separate the molecules by size in an open channel. Molecules with different size have different diffusivities and are located vertically in different positions when passing through an open channel. In this study, hollow fiber membranes instead of conventional rectangular channels have been used as materials for the open channel and this change would decrease the cost of manufacturing. FIFFF is a useful technique to characterize the biopolymeric materials. Retention time, diffusion coefficients and Stokes radius of analysis can be calculated from the related simple equations. Hollow-fiber flow field-flow fractionation (HF-FIFFF) has been used for the characterization and separation of protein mixture in a phosphate buffer solution and has demonstrated the potential to be developed into a disposable FIFFF channel. The important indexes for the analytical separation are selectivity, resolution and plate height. The optimized separation condition for protein mixture of Ovalbumin, Alcohol dehydrogenase, Apoferritin and Thyroglobulin is  $\dot{V}_{out}/\dot{V}_{rad} = 0.65/0.85$  mL/min.

**Key Words :** Hollow fiber flow FFF, Protein mixture, Retention time

### Introduction

Hollow fiber flow FFF (HF-FIFFF) is a new separation method for polymers and particles. As opposed to the normal arrangement with two parallel plates as a separation channel in Flow Field-Flow Fractionation (FIFFF), cylindrical hollow fiber FFF has certain advantages, such as simplicity of operation and independent control of the two flows (elution and cross flow), including an easier way of performing gradient elution. The cylindrical channel automatically maintains its cylindrical cross section when pressurized.<sup>1-4</sup>

Generally in FIFFF, a flat rectangular separation channel consisting of two parallel plates is used. The force field is a secondary flow of liquid (cross flow) going through the two channel walls and intersecting the elution flow. This equipment requires that both channel walls should be permeable.

FIFFF encompasses a large variety of methods of separation and characterization of supramolecular compounds (macromolecules, colloids, particles, cells). FIFFF experiments had already been conducted using a bundle of hollow fibers.<sup>5</sup> Jönsson and Carlshaf applied HF-FIFFF system to separation of polystyrene latex beads and studied the influence of ionic strength of the solvent and the properties of various types of fiber.<sup>6-9</sup> In 1995 Wijnhoven et al. applied the same HF-FIFFF system to separate polystyrene sulfonate and to investigate water-soluble polymers.<sup>10,11</sup>

Recently, it has been reported that particle separation by HF-FIFFF can be greatly increased to the resolution level normally achieved by a rectangular system of optimization.<sup>12</sup> Moreover it has been shown that hollow fiber can be a potential alternative to acquire particle Stokes diameter distribution provided that it is developed into a facilitated

and disposable module in HF-FIFFF. In this study, hollow fiber membranes instead of conventional rectangular channels have been used as materials for the open channel and this channel would decrease the cost of manufacturing. It has been demonstrated that HF-FIFFF is suited to the fractionation of proteins nanosized.

The characterization and separation of protein mixture in a phosphate buffer solution have been investigated in HF-FIFFF, and then HF-FIFFF has demonstrated for the potential to be developed into a disposable FIFFF channel.

### Theory

The FFF mechanism combines elements of chromatography and field-driven techniques such as electrophoresis and ultracentrifugation. Like chromatography, FFF is an elution technique with underlying roots in differential flow displacement and like field-driven techniques, FFF requires a field or gradient. Instead of utilizing a stationary phase as in chromatography, to achieve separation, FFF takes advantages of an external force field that is applied perpendicular to the separation channel.

Classical FFF utilizes force fields of various types, each with a unique interaction mechanism with the solute. The most common force fields are sedimentation field (SdFFF), secondary flow (FIFFF), and temperature gradient (TFFF). SdFFF out of these types has been most thoroughly investigated.<sup>13</sup> SdFFF utilizes a gravity field to separate particles according to their masses and densities. The rectangular-shaped channel is curved inwards to fit within the rotor basket of a centrifuge.<sup>14</sup>

FIFFF is the most universal of the FFF techniques. In this variant of FFF, a secondary flow is applied perpendicularly to the elution flow. Two parallel semipermeable plates form the channel. FIFFF differs from all other types of FFF in that

\*Corresponding author. Tel & Fax: +82-2-365-8570; E-mail: minbr345@yonsei.ac.kr

the retention parameter is a function of only one sample parameter, the diffusion coefficient. As a consequence, the elution volume for an unknown sample can directly be used to calculate the size of the molecule (Stokes' radius) without calibration. This is possible only if the surface properties of the sample and the channel wall are known.<sup>15-17</sup>

Particle retention in HF-FIFFF is further examined by comparing retention time with the theory in Eq. (1). In order to calculate the retention time  $t_R$  from Eq. (1), an accurate knowledge of efficient fiber radius must be known first. Experimentally, image of hollow fiber used in this work is obtained by cutting the frozen fiber after the immediate immersion into the liquid nitrogen.

$$t_R = \frac{r_f^2}{8D} \ln(\langle v \rangle(\zeta) / \langle v \rangle(L)) \quad (1)$$

Here,  $r_f$  and  $D$  are the hollow fiber radius and diffusion coefficient, respectively.  $\langle v \rangle(\zeta)$  and  $\langle v \rangle(L)$  are the mean axial flows in the beginning and at end of the fiber.

Resolution, like separation factor, differs for each specific component pair and therefore fails as global criterion of separation. For analytical separations, more universal criteria have evolved, such as plate height, number of plate, rate of plate generation, and peak capacity. The most important index for the analytical separation of two specific components is the resolution  $R_s$ . This parameter categorizes the overlap of two specific component zones. If the centers of gravity of the two zones are founded at locations  $X_1$  and  $X_2$ , respectively, then the resolution can be defined as<sup>19</sup>

$$R_s = \frac{2(X_2 - X_1)}{W_{b1} + W_{b2}} \quad (2)$$

where  $X$  is the peak retention volume,  $W_b$  is the peak width formed by intersection of the tangents to the curve inflection points with the baseline in retention volume units,  $W_b = 4\sigma$  and  $\sigma$  is the peak standard deviation (proportional to peak width).

The subscripts 1 and 2 serve to identify two closely eluting solutes. The plate height  $H$  is equal to  $L/N$ , where  $L$  and  $N$  are the column length and the number of plate, respectively.

Eq. (2) may also be written as

$$R_s = \frac{X_2 - X_1}{2(\sigma_1 + \sigma_2)} \quad (3)$$

Particle diameter,  $d$ , can be calculated by substituting the diffusion coefficient,  $D = kT/3\pi\eta d$  and the rearrangement results in

$$d = \left( \frac{t_{R1}}{t_R} \right)^{\frac{1}{s}} \quad (4)$$

where  $t_{R1}$  is the constant equal to the extrapolated value of  $t_R$  for particles of unit diameter and  $s$  is the selectivity of the slope of a calibration. Eq. (4) can be used for the particle Stokes diameter calculation from an experimental fractogram of a particle sample.

## Experimental Section

Hollow fiber membrane used in this work is PAN (polyacrylonitrile), having a molecular weight cut-off of 30,000 obtained from KMST (Korea). The hollow fiber separation module is prepared in the previous work.<sup>12</sup> The dimensions of hollow fiber module are 24 cm in length,  $L$ , and 0.442 mm (in dried condition) with radius  $r_f$ . Carrier liquid is prepared by ultra pure water containing 0.25 mM phosphate (Sigma chemical co., USA) buffer solution for particle dispersion. Carrier solution is delivered to the hollow fiber module by an HPLC pump from Younglin Instrument (Seoul, Korea). Table 1 is proteins (Sigma chemical co., USA) used this work. A Model M720 UV detector from Younglin Instrument detects the eluted samples at 280 nm wavelength. The detector signal is collected by a PC using the Autochro-Win data acquisition software from Younglin.

Followed by the sample injection, the focusing/relaxation process is carried out by delivering the carrier liquid into both fiber inlet and outlet. The focusing process is accomplished with a single pump by splitting flow into two parts (delivered to both inlet and outlet). The flow rate adjustment for the outflow and radial flow is made with a same SS-SS2-VH Nupro metering valve from Nupro Co. (Willoughby, OH, USA).

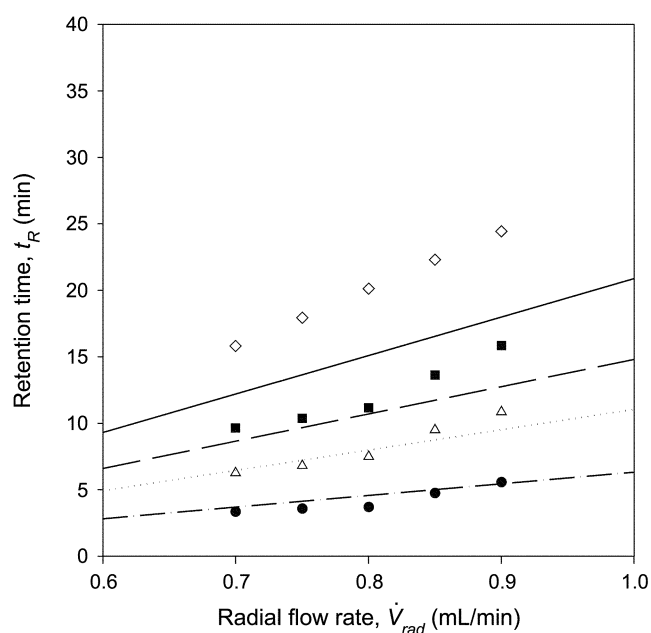
## Results and Discussion

Figure 1 shows the experimental results and theoretically calculated values of the retention time as a function of the radial flow rate, with the phosphate buffer solution as the carrier. Experimental data points are represented as symbols. The dotted lines are the calculated retention time based on the measured radius ( $r_f = 0.44$  mm) of swollen fiber. Data points appear to lie above the theoretical line throughout the axial flow rate conditions examined in this work. It means that the retention of particles is longer at practice than at theory. The deviations from the theory may imply that there

**Table 1.** Properties of Protein

| Protein               | MW      | pI      | Stokes diameter (nm) | Source       | Size (Å)           |
|-----------------------|---------|---------|----------------------|--------------|--------------------|
| Ovalbumin             | 44,287  | 4.9     | 5.2                  | Chicken egg  | 62.9 × 84.7 × 71.5 |
| Alcohol dehydrogenase | 150,000 | 5.4-5.8 | 9.1                  | Yeast        | 50.6 × 44.1 × 92.6 |
| Apo ferritin          | 444,000 | 5.0     | 12.2                 | Horse spleen | 184 × 184 × 184    |
| thyroglobulin         | 669,000 | 5.1     | 17.2                 | Bovine       | ND*                |

ND\* : non-data



**Figure 1.** Plot of retention time vs. radial flow rate ( $\dot{V}_{rad}$ ) of proteins. Symbols are the experimental data points: ● (ovalbumin), △ (alcohol dehydrogenase), ■ (apoferritin), ◇ (thyroglobulin). The linear lines are theoretical retention time calculated from the radius.

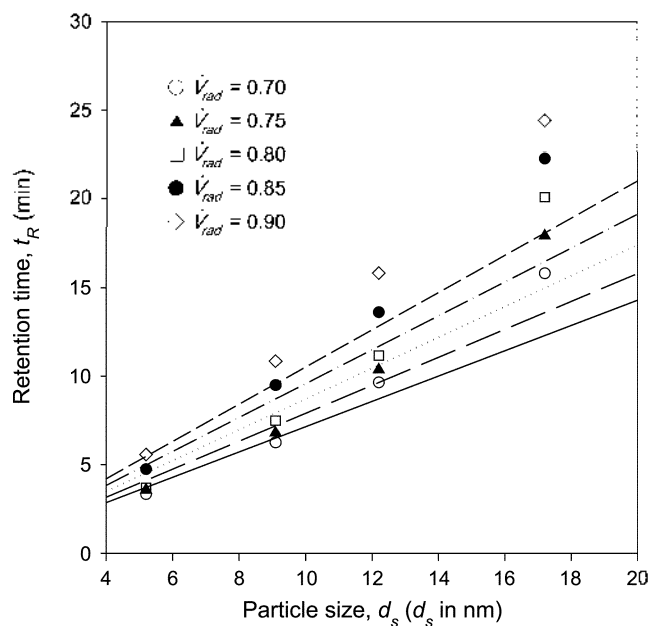


**Figure 2.** Experimental (point) and theoretically calculated values (lines) of retention time ( $t_R$ ) vs. particle Stokes diameter ( $d_s$ ):  $\dot{V}_{in} = 1.5$  mL/min.

somehow exists the possibility of fiber expansion under the pressure given by the system.

In Figure 3, the logarithm of retention time of four proteins is plotted as symbols against the logarithm of particle Stokes diameter instead of algebra in Figure 2. The solid and dotted lines represent the semi empirical theoretical values. The data points for the large diameter size appear to be deviated from the theoretical values calculated by Eq. (1).

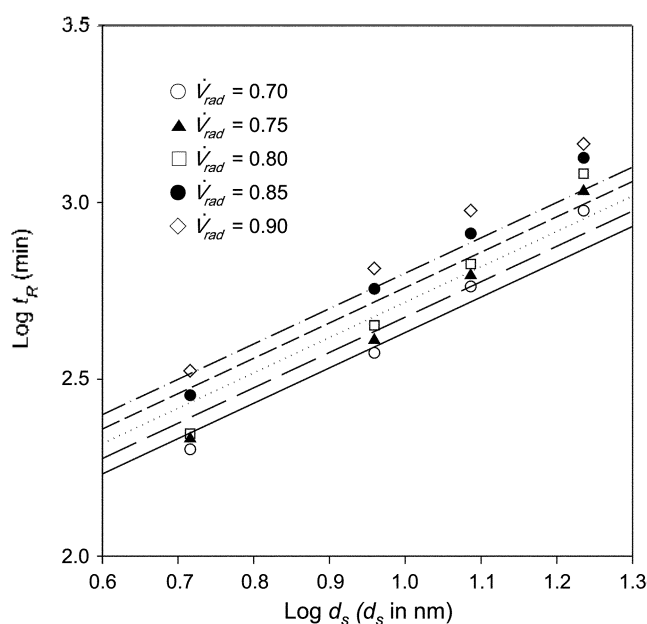


**Figure 3.** Plot of  $\log t_R$  vs.  $\log d_s$  of proteins obtained at different axial flow rate conditions.  $\dot{V}_{in}$  for all runs is 1.5 mL/min. The linear lines are calculated on the basis of each calibrated radius.

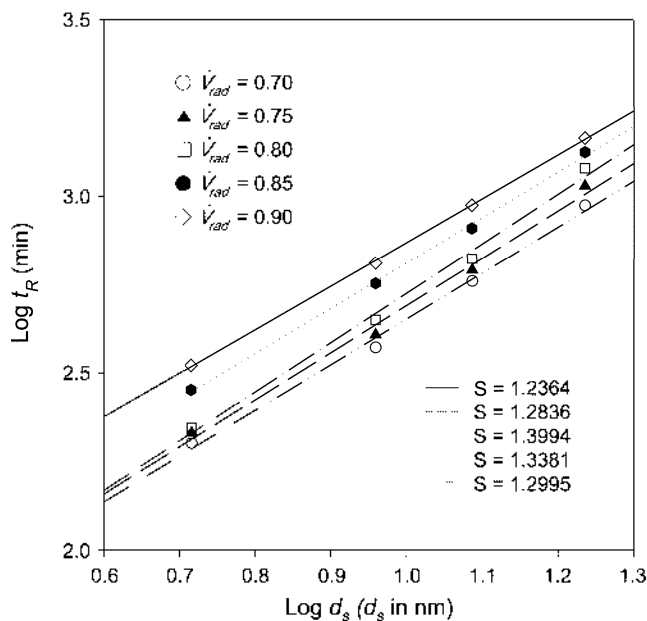
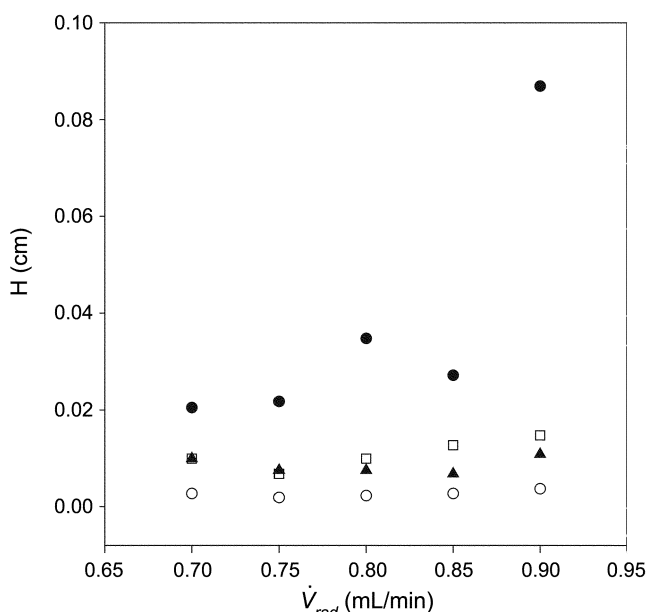


**Figure 4.** Plot of  $\log t_R$  vs.  $\log d_s$  for proteins at different radial flow rate conditions. Run condition is fixed at  $\dot{V}_{in} = 1.5$  mL/min.

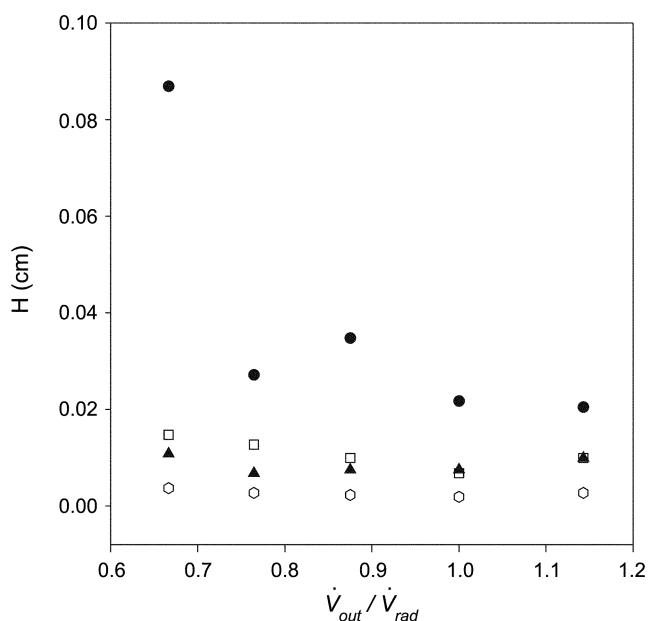
The difference between the observed and theoretical retention times is because of the increasing steric effect of large particles by the growing field strength.

Figure 4 shows a plot of logarithmic retention time versus  $\dot{V}_{rad}$  for a mixture of proteins eluted using PAN hollow fiber membrane. Slope of the lines is the selectivity of membrane.

In this work, the selectivity of hollow fiber membrane is 1.24-1.4. The typical selectivity value is approximately 1.5 in flow FFF whereas it is 0.7-0.8 for sedimentation FFF runs.<sup>18,19</sup> The high selectivity values means that particle



**Figure 5.** The measured plate height vs.  $\dot{V}_{rad}$  for four proteins: ○ (ovalbumin), ▲ (alcohol dehydrogenase), □ (apoferritin), ● (thyroglobulin).



**Figure 6.** Plate height vs.  $\dot{V}_{out}/\dot{V}_{rad}$ : ○ (ovalbumin), ▲ (alcohol dehydrogenase), □ (apoferritin), ● (thyroglobulin).

separation in normal mode by HF-FIFFF is suitable for multi-component separation.

The experimentally obtained plate heights are shown in Figure 5-6. Here, the experimental plate height data is plotted against the radial flow rate for four proteins. The difference increases according to the radial flow.

The tendency between plate height and radial flow rate appears to vary. It is believed that the main reason for discrepancy is the initial distribution of sample. In experiments, the initial distribution of sample at the end of

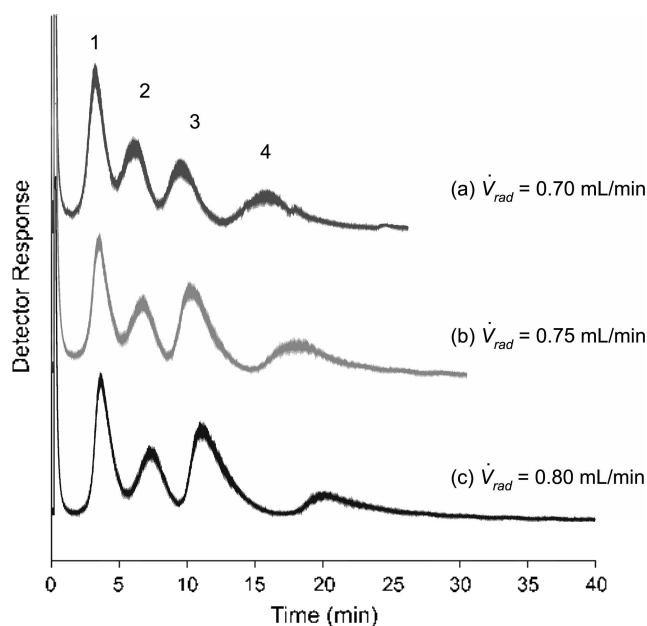


**Figure 7.** Influence of elution profile according to varying radial flow rate; (a)  $\dot{V}_{rad} = 0.70$  mL/min, (b)  $\dot{V}_{rad} = 0.75$  mL/min, (c)  $\dot{V}_{rad} = 0.80$  mL/min; protein 1 (Ovalbumin), 2 (Alcohol dehydrogenase), 3 (Apoferritin), 4 (Thyroglobulin).

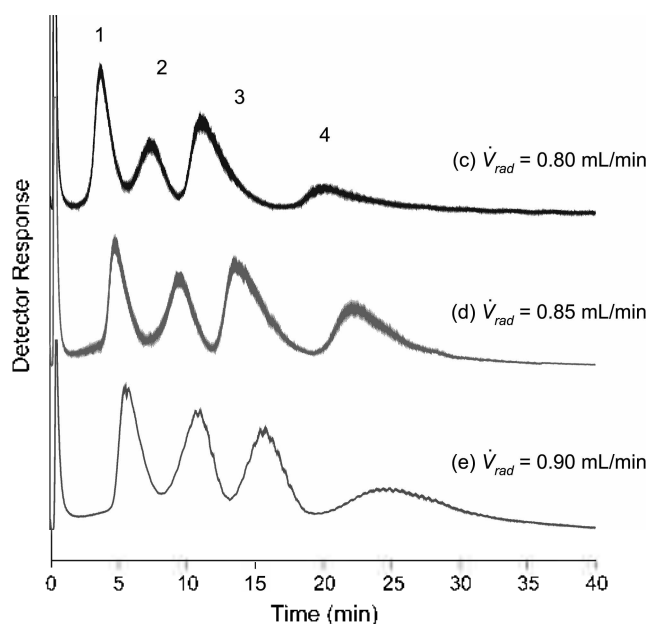


**Figure 8.** Influence of elution profile according to varying radial flow rate: (c)  $\dot{V}_{rad} = 0.80$  mL/min, (d)  $\dot{V}_{rad} = 0.85$  mL/min, (e)  $\dot{V}_{rad} = 0.90$  mL/min; protein 1 (Ovalbumin), 2 (Alcohol dehydrogenase), 3 (Apoferritin), 4 (Thyroglobulin).

relaxation brings about broadening of initial sample zone and it increases peak standard deviation, which fatally influences plate height. This results in increasing plate height. The similar result was already reported at the rectangular channel by Wahlund.<sup>20</sup>

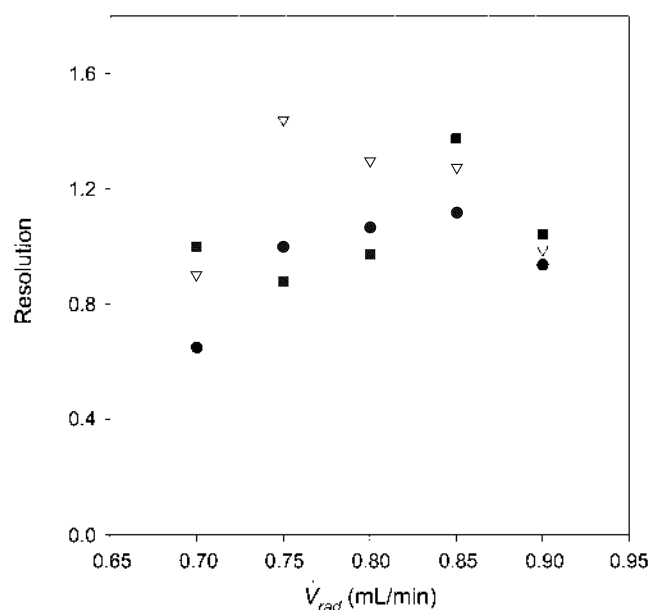
Figure 6 shows the plot of plate height against ratio  $\dot{V}_{out}/\dot{V}_{rad}$  for various  $\dot{V}_{out}$ . It is one of the proofs of

performances of the hollow fiber membrane channel.

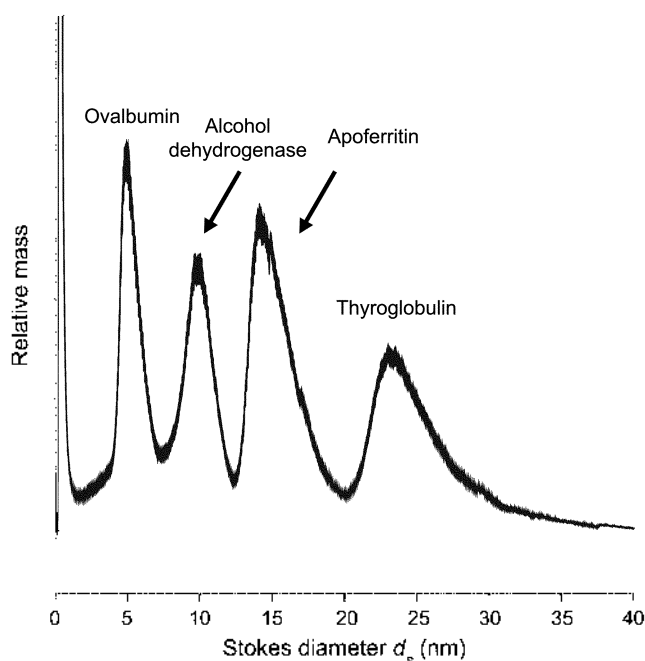
Figure 7 and 8 show the elution profile of protein mixtures obtained by varying radial flow rate, and analysis was done with UV detector. All runs were made at  $\dot{V}_{in} = 1.5$  mL/min and at the room temperature. As the radial flow rate is increased, the retention time is slightly shifted. Weak field strength and quick axial flow rate are required if it is necessary to analyze mixture fast. As the field strength is strong, the shape of the profile gets disturbed especially in  $\dot{V}_{out} = 0.6$  mL/min. At radial flow rate  $\dot{V}_{rad} = 0.7$ - $0.8$  mL/min, the peaks are not clearly separated. When the radial flow rate ( $\dot{V}_{rad}$ ) is elevated  $0.85$  mL/min, all peaks are clearly separated. But when the radial flow rate ( $\dot{V}_{rad}$ ) is further elevated to  $0.90$  mL/min, it seems that the resolution of the peaks is decreased. This is due to the increase of the experimental retention ratio, which results in the increase of nonequilibrium band broadening in the FFF procedure. It seems to result from the interaction between sample and the channel accumulation wall. The high radial flow rate concerns that particle will be driven so forcefully to the channel accumulation wall that they will adhere to the wall and thus fail to elute. From the results, we know that separation of more mixed particles is done under low ratio of axial flow to radial flow and high field strength.

Figure 9 shows the resolution vs. radial flow rate for all operations is  $\dot{V}_{in} = 1.5$  mL/min. For the clear separation of two peaks, the resolution  $R_s$  is more than 1.5 when the peak is a Gaussian peak. The resolution of the PAN membrane is 1.118-1.375 among four proteins.

When the radial flow rate condition is  $0.85$  mL/min, the resolution is the largest. Under these conditions, the mixture is completely separated. The optimized separation condition



**Figure 9.** Plot of resolution data vs. radial flow rate. For all runs  $\dot{V}_{in} = 1.5$  mL/min. Resolution is measured between particle and particle; ■ (between Ovalbumin and Alcohol dehydrogenase), ● (between Alcohol dehydrogenase and Apoferritin), ▽ (between Apoferritin and Thyroglobulin).



**Figure 10.** Fractogram of particle Stokes diameter distribution. The HF-FIFFF run obtained at  $\dot{V}_{out}/\dot{V}_{rad} = 0.65/0.85$ . PAN hollow fiber membrane.

is  $\dot{V}_{out}/\dot{V}_{rad} = 0.65/0.85$  mL/min.

The run condition of fractogram of the proteins is  $\dot{V}_{out}/\dot{V}_{rad} = 0.65/0.85$  mL/min. The particle Stokes diameter calculation is made for the fractogram signal by using Eq. (2).

The resulting particle Stokes diameter distribution (PSD) is shown in Figure 10.

## Conclusions

In this work, it has been demonstrated that HF-FIFFF is suitable for the fractionation of nano-sized proteins. With a separation performance comparable to that reported in literature for convenient FIFFF, HF-FIFFF appears to be more convenient for several reasons. First, the cost of the HF-FIFFF channels is very low, even in comparison with a single membrane for conventional FIFFF. Secondly, even though HF-FIFFF proved to be quite reproducible within multiple runs, low cost and simplicity potentially allow for single-run, disposable usage.

The result observed in this work is as follows

1. Experimental data appears to lie above the theoretical line throughout the axial flow rate conditions examined in this work. It means particles retain longer than they are expected by the theory. The deviations from the theory may imply that there somehow exists the possibility of particle aggregation under the pressure given by the system.

2. The slope of the lines is the selectivity of membrane and the selectivity of hollow fiber membrane is 1.24-1.4. The high selectivity values means that particle separation in normal mode by HF-FIFFF is suitable for multi-component separation.

3. The important index of success for the analytical separation of two specific components is the resolution  $R_s$ . The resolution of the PAN membrane is 1.118-1.375 among four proteins. When the radial flow rate condition is 0.85 mL/min, the resolution is the largest. Under these conditions, the mixture is completely separated. The optimized separation condition for protein mixture of Ovalbumin, Alcohol dehydrogenase, Apoferritin and Thyroglobulin is  $V_{out}/V_{rad} = 0.65/0.85$  mL/min.

HF-FIFFF is feasible and can be described theoretically with reasonable accuracy. The concept is technically simple and the experimental parameters involving field gradient elution can be controlled independently, which permits flexible operation.

**Acknowledgments.** This work was supported by grant No. R01-2001-000-00420-0 from the Korea Science & Engineering Foundation and BK21.

### References

1. Bruijjsvoort, M.; Kok, W. T.; Tijssen, R. *Anal. Chem.* **2001**, *73*, 4736.
2. Giddings, J. C. *Science* **1993**, *260*, 1456.
3. Moon, M. H.; Hwang, I. *J. Liq. Chrom. & Rel. Technol.* **2001**, *24*, 3069.
4. Schimpf, M. E.; Caldwell, K.; Giddings, J. C. *Field-flow Fractionation Handbook*; Wiley-Interscience: New York, U. S. A., 2000.
5. Lee, H. L.; Reis, J. F. G.; Dohner, J.; Lightfoot, E. N. *AIChE. J.* **1974**, *20*, 776.
6. Jönsson, J. Å.; Carlshaf, A. *Anal. Chem.* **1989**, *61*, 11.
7. Carlshaf, A.; Jönsson, J. Å. *Sep. Sci. Tech.* **1993**, 1191.
8. Carlshaf, A.; Jönsson, J. Å. *J. Microcol. Sep.* **1991**, *3*, 411.
9. Carlshaf, A.; Jönsson, J. Å. *Sep. Sci. Tech.* **1993**, *28*, 1031.
10. Wijnhoven, J. E. G. J.; Koon, J. P.; Poppe, H.; Kok, W. T. *J. Chromatogr.* **1995**, *699*, 119.
11. Wijnhoven, J. E. G. J.; Koon, J. P.; Poppe, H.; Kok, W. T. *J. Chromatogr.* **1996**, *732*, 307.
12. Lee, W. J.; Min, B. R.; Moon, M. H. *Anal. Chem.* **1999**, *71*, 3449.
13. Myers, M. N.; Caldwell, K. D.; Giddings, J. C. *Sep. Sci.* **1974**, *9*, 47.
14. Giddings, J. C.; Yang, F. J. F.; Myers, M. N. *Anal. Chem.* **1976**, *48*, 1126.
15. Giddings, J. C. *Sep. Sci.* **1966**, *1*, 3.
16. Granger, J.; Dodds, J.; Leclerc, D.; Midoux, N. *Chem. Eng. Sci.* **1986**, *41*, 3119.
17. Walund, K. G.; Giddings, J. C. *Anal. Chem.* **1987**, *59*, 1332.
18. Williams, P. S.; Moon, M. H.; Xu, Y.; Giddings, J. C. *Chem. Eng. Sci.* **1996**, *51*, 4477.
19. Yau, W. W.; Kirkland, J. J.; Bly, D. D. *Modern Size-Exclusion Liquid Chromatography*; Wiley-Interscience: New York, U. S. A., 1979.
20. Williams, P. S.; Kosh, T.; Giddings, J. C. *Chem. Eng. Column.* **1998**, *111*, 121.